CLIMATOLOGY

Warming homogenizes apparent temperature sensitivity of ecosystem respiration

Ben Niu[1,2], Xianzhou Zhang[1,3]*, Shilong Piao[4,5], Ivan A. Janssens[6], Gang Fu[1], Yongtao He[1,3], Yangjian Zhang[1,3], Peili Shi[1,3], Erfu Dai[1], Chengqun Yu[1], Jing Zhang[7], Guirui Yu[1,3], Ming Xu[1], Jianshuang Wu[8], Liping Zhu[5], Ankur R. Desai[9], Jiquan Chen[10], Gil Bohrer[11], Christopher M. Gough[12], Ivan Mammarella[13], Andrej Varlagin[14], Silvano Fares[15], Xinquan Zhao[16], Yingnian Li[16], Huiming Wang[1], Zhu Ouyang[1]

Warming-induced carbon loss through terrestrial ecosystem respiration (*Re*) is likely getting stronger in high latitudes and cold regions because of the more rapid warming and higher temperature sensitivity of *Re* (Q_{10}). However, it is not known whether the spatial relationship between Q_{10} and temperature also holds temporally under a future warmer climate. Here, we analyzed apparent Q_{10} values derived from multiyear observations at 74 FLUXNET sites spanning diverse climates and biomes. We found warming-induced decline in Q_{10} is stronger at colder regions than other locations, which is consistent with a meta-analysis of 54 field warming experiments across the globe. We predict future warming will shrink the global variability of Q_{10} values to an average of 1.44 across the globe under a high emission trajectory (RCP 8.5) by the end of the century. Therefore, warming-induced carbon loss may be less than previously assumed because of Q_{10} homogenization in a warming world.

INTRODUCTION

Terrestrial ecosystem respiration (*Re*), the sum of autotrophic respiration from primary producers and heterotrophic respiration from consumers and detritivores, represents a fundamental biospheric function and plays a major role in the global carbon cycle and growth rate of atmospheric CO_2 (*1*). However, Earth system models currently in use poorly simulate the temporal variability of *Re* compared with in situ observations (*2*, *3*), with model performance differing substantially among biomes and latitudes (*4*–*7*). Thus, future *Re* dynamics are poorly constrained and difficult to evaluate (*7*–*11*). Discrepancies between modeled and observed *Re* are often attributed to inaccuracies in the parameterized temperature sensitivity of ecosystem respiration (Q_{10}) (*9*, *12*). Actually, difference in parameterized Q_{10} is partially due to the misunderstanding of Q_{10} from field ecologists and mechanistic modelers (*12*). Early-generation models interpreted respiration as a temperature-dependent process in which Q_{10} was often set at a constant value, typically 2 (*8*, *13*), i.e., *Re* doubles for a 10°C rise in temperature. However, recent studies have suggested that a constant Q_{10} is inadequate to predict *Re* because the processes involving plants and soil across time and space are not the same (*11*, *14*–*16*). In contrast, field observations focus more on the apparent Q_{10}, the observable ecosystem response of *Re* to temperature that arises from the combination of multiple processes, each with their own temperature sensitivities. These studies have shown that Q_{10} decreases with increasing temperature and is thus higher in ecosystems at higher latitudes and in colder regions (*17*). Moreover, global warming rates are highly heterogeneous, with higher latitudes warming faster than lower latitudes. The joint consideration of faster warming and higher Q_{10} at high latitudes and cold regions implies a much stronger carbon efflux–climate warming feedback from these ecosystems (*18*). Although the spatial relationship between temperature and Q_{10} has been well established in terrestrial ecosystems, the temporal change in Q_{10} in response to ongoing global warming has not yet been studied at depth across the globe.

Knowledge of how Q_{10} will change with future climate warming can be investigated through two different pathways. One is through manipulative field warming experiments (*2*, *18*), which provide direct, quantitative evidence of site-specific ecosystem responses to warming. Unfortunately, these experiments are hard to conduct at a relevant large scale and are therefore rare. The few existing experiments varied in experimental designs and were often applied to specific respiration components or biospheric components, (e.g., soil warming only and soil respiration only) at small temporal and spatial scales, resulting in some important biomes being neglected. These experiments also carried high uncertainty because of the inherently low degree of replication and to inconsistent warming protocols (*19*). As a result, it is very difficult to quantify the global-scale impact of climate warming on Q_{10} over a long time frame using aggregated data from diverse field warming experiments.

An alternative approach is through space-for-time substitution, an indirect approach that relates the contemporary spatial pattern of Q_{10} to the ambient, climatic spatial temperature gradient to infer

[1]Key Laboratory of Ecosystem Network Observation and Modeling, Institute of Geographic Sciences and Natural Resources Research, Chinese Academy of Sciences, Beijing 100101, China. [2]University of Chinese Academy of Sciences, Beijing 100049, China. [3]College of Resources and Environment, University of Chinese Academy of Sciences, Beijing 100190, China. [4]College of Urban and Environmental Sciences, Peking University, Beijing 100871, China. [5]Institute of Tibetan Plateau Research, Chinese Academy of Sciences, Beijing 100085, China. [6]Department of Biology, University of Antwerpen, Universiteitsplein 1, Wilrijk B-2610, Belgium. [7]College of Global Change and Earth System Science, Beijing Normal University, Beijing 100875, China. [8]Institute of Environment and Sustainable Development in Agriculture, Chinese Academy of Agricultural Sciences, 100081 Beijing, China. [9]Department of Atmospheric and Oceanic Sciences, University of Wisconsin-Madison, Madison, WI 53706, USA. [10]Department of Geography, Michigan State University, East Lansing, MI 48823, USA. [11]Department of Civil, Environmental and Geodetic Engineering, The Ohio State University, Columbus, OH 43210, USA. [12]Department of Biology, Virginia Commonwealth University, Richmond, VA 23284-2012, USA. [13]Institute for Atmospheric and Earth System Research/Physics, Faculty of Science, University of Helsinki, P.O. Box 68, Helsinki FI-00014, Finland. [14]A.N. Severtsov Institute of Ecology and Evolution, Russian Academy of Sciences, Moscow 119071, Russia. [15]National Research Council of Italy, Institute of BioEconomy, Via dei Taurini 19, 00100 Rome, Italy. [16]Northwest Institute of Plateau Biology, Chinese Academy of Sciences, Xining 810001, China.
*Corresponding author. Email: zhangxz@igsnrr.ac.cn

the likely response of Q_{10} to climate warming (*8*). This approach has been widely used as a compromise when observational time series do not cover a large-enough temperature gradient in developing a temperature response function for measured Q_{10} (*8*, *20*). However, the adequacy of space-for-time substitution was rarely tested (*8*). The advent and advancement of long-term carbon flux monitoring stations allow us to test this approach on estimation of Q_{10}. In this study, we used standardized long-term eddy covariance (EC) observations from diverse climates and biomes worldwide to (i) identify Q_{10} changes and their underlying mechanisms along temporal and spatial temperature gradients, (ii) test the adequacy of space-for-time substitution in the analyses of Q_{10} patterns, and (iii) predict changes in spatial patterns of Q_{10} under future climate warming scenarios.

RESULTS

We extracted long-term time series of half-hourly *Re* and meteorological data from the global network of FLUXNET sites. All available half-hourly data were gathered, but sites with less than 5 years data were excluded. If more than 25% of 1-year data or if continuous observations for more than 1 month were missing from a site, that particular site-year was excluded from further analysis completely (detailed data filtering is described in Materials and Methods). As a result, a set of 74 sites (604 site-years; table S1) was used to derive Q_{10} values for each site-year ($Q_{10\,year,site}$) (Eqs. S1 and S2, Materials and Methods). We introduced priori tests for temperature and moisture effects on $Q_{10\,year,site}$. Our results showed that moisture did not significantly influence $Q_{10\,year,site}$ when considering the temperature effects on $Q_{10\,year,site}$ (fig. S1 and see Materials and Methods). Therefore, in this study, we chose to focus only on the effect of temperature on Q_{10}.

We found that $Q_{10\,year,site}$ was negatively correlated with annual mean air temperature at the site ($T_{year,site}$) across almost all sites (slopes of dashed lines in Fig. 1A), implying lower $Q_{10\,year,site}$ in warmer years for the majority (95%) of sites. To understand the long-term (years to decades) $Q_{10\,year,site}$ response to temperature variation, we identified the temporal temperature sensitivity of $Q_{10\,year,site}$ ($\delta_{temporal}$), i.e., the change in $Q_{10\,year,site}$ per 1°C change in $T_{year,site}$, which we calculated from the regression slope between $Q_{10\,year,site}$ and $T_{year,site}$ at individual sites (Materials and Methods and Fig. 1A). We found that $\delta_{temporal}$ was significantly and positively correlated with annual mean site temperature ($T_{\overline{year},site}$) ($P < 0.0001$) (red line in Fig. 1B), exhibiting larger warming-induced declines in $Q_{10\,year,site}$ at colder sites than at warmer sites. Specifically, $\delta_{temporal}$ at the colder arctic and boreal sites was more negative (average: −0.39; 95% confidence interval (CI): −0.51 to −0.26) than those at temperate (−0.11; CI: −0.14 to −0.08) and (sub-)tropical sites (−0.10; CI: −0.13 to −0.06) (table S2).

Our analyses thus revealed strong support for a lower Q_{10} in a warmer world, with larger declines occurring in colder climate regions where Q_{10} is presently higher, and smaller reductions where Q_{10} is presently lower. As a result, the global variability of Q_{10} is likely to shrink in response to the ongoing global warming, especially given the stronger warming trend in the colder regions. Unfortunately, this analysis did not allow for extrapolation to a future, much warmer climate because the current interannual range of long-term mean annual temperature change at individual sites (typically about 1° to 3°C) did not encompass the projected values expected under future warming. However, the spatial gradient of Q_{10} did encompass a large enough temperature change range, and for this reason, a space-for-time substitution would provide more insight into how Q_{10} might change with pronounced future warming. Therefore, we investigated site-specific $Q_{10\,\overline{year},site}$, calculated as the arithmetic mean of all $Q_{10\,year,site}$ values among all study years at individual sites.

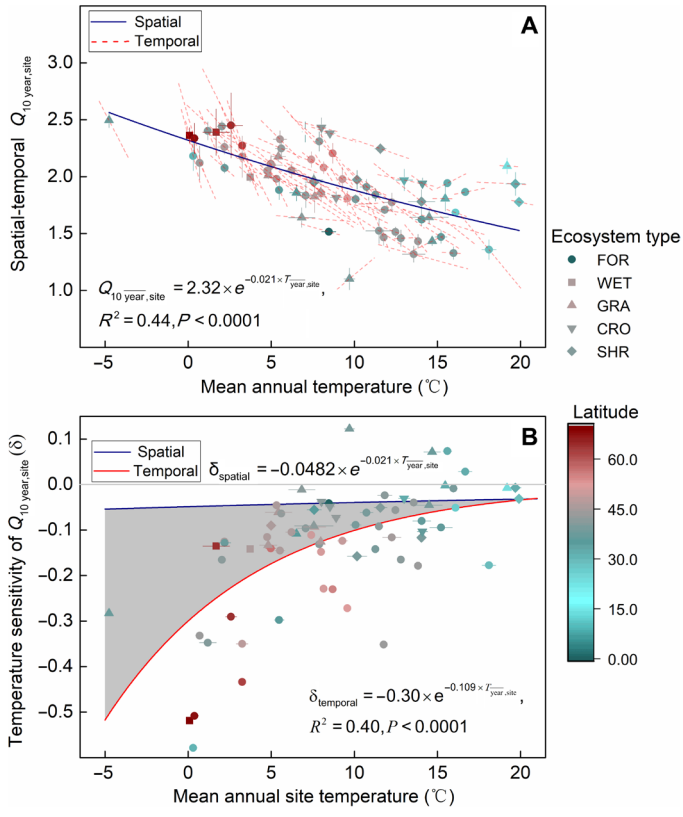

Fig. 1. Spatio-temporal patterns of Q_{10} and its temperature sensitivity against mean annual temperature through time and across space. In (**A**), the points show annual mean Q_{10} values at individual sites ($Q_{10\,\overline{year},site}$). The red dashed lines represent how annual $Q_{10\,year,site}$ values vary temporally at individual sites. The blue solid line represents the exponential regressions of spatial $Q_{10\,\overline{year},site}$ against temperature. In (**B**), the points show site-specific $\delta_{temporal}$ that are the linear slopes of the temporal regression of Q_{10} [red dashed lines in (A)] against temperature. The red line is an exponential fitting of $\delta_{temporal}$ along temperature. The blue solid line is the first derivative curve of the contemporary spatial regression of Q_{10} in (A) (blue line) ($\delta_{spatial}$). The shadow represents the difference between $\delta_{spatial}$ and $\delta_{temporal}$. Sites are grouped by ecosystem types according to the International Geosphere Biosphere Programme (IGBP) classification (Materials and Methods). The colored band shows the latitudinal position of the individual sites. Error bars are the standard error of the corresponding mean values.

$Q_{10\,\overline{year},site}$ varied between 1.1 and 2.5, with an overall arithmetic mean of 1.94 (95% CI: 1.87 to 2.01) (Fig. 1A and tables S1 and S2). No significant differences in $Q_{10\,\overline{year},site}$ were detected among ecosystem types ($P > 0.1$). However, significant differences in $Q_{10\,\overline{year},site}$ were found among climatic regions ($P < 0.0001$) (table S2). Arctic and boreal regions generally had greater $Q_{10\,\overline{year},site}$ values than temperate regions, which in turn exhibited higher $Q_{10\,\overline{year},site}$ values than subtropical and tropical regions (table S2). Spatially, $Q_{10\,\overline{year},site}$ significantly and exponentially decreased with increasing $T_{\overline{year},site}$ ($R^2 = 0.44$, $P < 0.0001$; Fig. 1A), consistent with the negative temperature dependency of the temporal $Q_{10\,year,site}$ at individual sites.

Based on this contemporary distribution of $Q_{10\,\overline{year},site}$ across the spatial temperature gradient, we derived the spatial temperature sensitivity of $Q_{10\,\overline{year},site}$ ($\delta_{spatial}$), i.e., the change in $Q_{10\,\overline{year},site}$ per 1°C change in $T_{\overline{year},site}$, from the derivative of the exponential relationship between $Q_{10\,\overline{year},site}$ and $T_{\overline{year},site}$ for each site-specific annual mean temperature (Materials and Methods). Compared with $\delta_{temporal}$, $\delta_{spatial}$ showed a consistent temperature-dependent trend and was more negative at higher latitudes and in colder regions (Fig. 1B and table S2). However, the magnitude of $\delta_{spatial}$ was significantly lower than that of $\delta_{temporal}$ in all climatic regions, especially in colder climates (Fig. 1B and table S2). Therefore, as applied here, the space-for-time substitution substantially underestimated the decline of $Q_{10\,\overline{year},site}$ with climate warming, at least in the current-day period, and especially at high latitudes and in cold regions.

While this systematic difference between Q_{10} derived through time series and that derived through space-for-time substitution might be real, it could also be an artifact introduced by the use of different biomes or different temperature ranges during their respective fitting processes. We therefore first tested whether the mixing of biomes in the space-for-time substitution influenced the Q_{10} estimates. Specifically, we estimated Q_{10} on the basis of a series of specific temperature ranges (STRs) and tested how Q_{10} varied spatially while controlling for temperature (Materials and Methods). Results showed that the negative spatial correlation between $Q_{10\,\overline{year},site}$ and site temperature (Fig. 1A) is no longer significant when the same temperature ranges are used for all sites (Fig. 2, A to J). However, the mean Q_{10} values at different specific temperature bins [$Q_{10,str(i\text{-}j)}$, $4°C \le i, j \le 23°C$] are significantly correlated with average measurement temperature ($P < 0.0001$) (Fig. 2), which is consistent with the negative spatial correlation between $Q_{10\,\overline{year},site}$ and site temperature (Fig. 1A). Thus, site-specific temperature was crucial in determining the spatial variation of $Q_{10\,\overline{year},site}$, while the geographical locations or biome type of the observational sites was not (Fig. 2, fig. S3, and table S2; Materials and Methods).

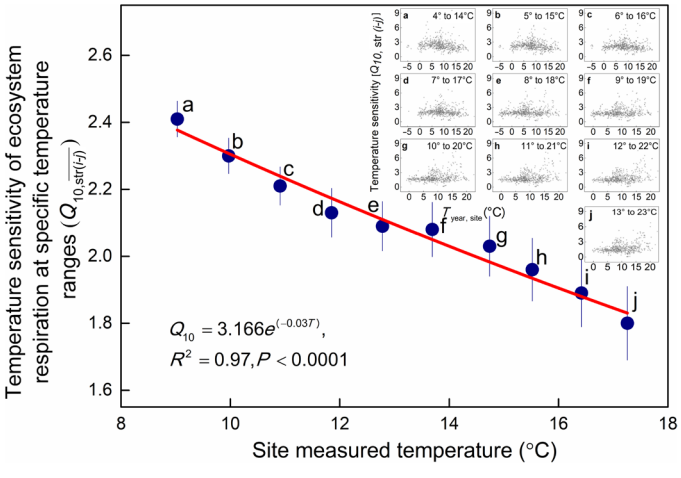

Fig. 2. The spatial trend of Q_{10} estimation in STRs ($Q_{10,\overline{str(i\text{-}j)}}$) against site measured temperature gradient. The inset graphs show Q_{10} estimation in STRs [$Q_{10,str(i\text{-}j)}$] from 4° to 23°C by a 10°C moving window (for more temperature moving window in fig. S3). The central blue dots are the arithmetic mean of the $Q_{10,str(i\text{-}j)}$ values ($Q_{10,\overline{str(i\text{-}j)}}$) with standard error (bars) for these 10 groups' STRs (**A** to **J**), and the red line is an exponential fit for their relationship with temperature.

We calculated $\delta_{temporal}$ using much smaller differences in mean annual temperature (generally <3°C) than were used in estimating $\delta_{spatial}$ (about 25°C across all sites, from −5° to 20°C; Fig. 1A), which may also have reduced the comparability of these indicators. To test whether the large difference between $\delta_{temporal}$ and $\delta_{spatial}$ originated from temperature ranges, we additionally estimated $\delta_{spatial}$ values for the smaller temperature ranges equivalent to those used in the temporal estimate, reducing the spatial temperature change window from 25° to 2°C (in 1°C steps; Materials and Methods). Subsequently, we calculated the $\delta_{spatial}$ values for all sites across all temperature ranges from 25° to 2°C (Fig. 3A, figs. S4 and S5, and table S3). In our dataset, the interannual mean temperature changes were generally <3°C (Fig. 1A); thus, we grouped $\delta_{temporal}$ of all sites into three groups of approximately 1°, 2°, and 3°C interannual temperature changes (Materials and Methods). We then tested the agreement between $\delta_{temporal}$ and $\delta_{spatial}$ values obtained from the same temperature range and the same sites. We found no significant differences between $\delta_{temporal}$ and $\delta_{spatial}$ when their associated temperature changes were similar (figs. S4 and S5). These results suggest that the space-for-time substitution required to project Q_{10} changes under future climate change is valid, but only if the temperature changes through time and across space are at comparable magnitude.

We further analyzed the change in $Q_{10\,\overline{year},site}$ under future warming conditions using space-for-time substitution at comparable temporal and spatial temperature change magnitudes. We extracted site-specific outputs of warming projections obtained from the Coupled Model Inter-comparison Project (CMIP5) under all Representative Concentration Pathway scenarios (RCPs; 2.6, 4.5, 6.0, and 8.5) until the end of the 21st century (2081–2100) (*21*) as nonequal warming scenarios (table S1; see Materials and Methods also for equal warming scenarios across sites). Using space-for-time substitution and the site-specific nonequal warming scenarios from RCP 2.6 to RCP 8.5, respectively (table S3 and fig. S6, Eq. S5 in Materials and Methods), we found that the curves of the best-fitting exponential regression for $Q_{10\,\overline{year},site}$ and $T_{\overline{year},site}$ became increasingly flatter as climate warming intensified (Fig. 3B). This result is consistent with homogeneous warming scenarios (fig. S7, A to E). Subsequently, $Q_{10\,\overline{year},site}$ gradually converged to a global average of 1.44 (95% CI: 1.38 to 1.50) for the RCP 8.5 warming scenario (Fig. 3B and fig. S7, F to I), a value over 25% lower and less spatially variable than the current global average of 1.94. In addition, the magnitude of $\delta_{spatial}$ consistently decreased with rising temperature, especially in colder regions (Fig. 3A), suggesting a progressive decline in the spatial difference in $\delta_{spatial}$ under ongoing warming. Clearly, future warming is likely to homogenize global $Q_{10\,\overline{year},site}$.

DISCUSSION

Several mutually nonexclusive mechanisms have been postulated to explain the lower Q_{10} values at higher temperatures. Manipulative field warming experiments (*2*, *17*, *22*), incubation experiments (*14*), bio-kinetics theory (*8*), and modeling studies (*23*) have suggested that Q_{10} is likely to decline with increasing temperature because of ecosystem thermal acclimation, either through biochemical (e.g., declining increase in molecules that have sufficient energy to overcome enzyme activation energies at increasing temperatures) or through structural changes (e.g., in community composition or reduced microbial biomass) (*22*–*24*). Other studies have provided

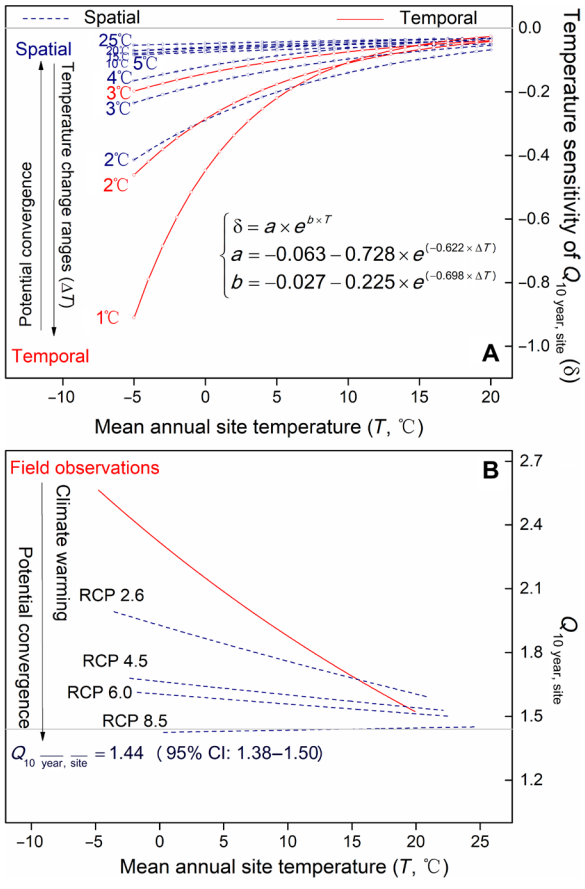

Fig. 3. Potential convergence in temperature sensitivity of ecosystem respiration under climate warming. In (**A**), all lines show the spatial patterns in temperature sensitivity of Q_{10} (δ) against site temperature across different temperature change ranges: blue dashed lines are the spatial δ ($\delta_{spatial}$) (fig. S4 and table S3, Materials and Methods), and red solid lines are temporal δ when the interannual temperature change ranges are approximately 1°C ($\delta_{temporal,1°C}$), 2°C ($\delta_{temporal,\ 2°C}$), and 3°C ($\delta_{temporal,\ 3°C}$), respectively (fig. S5 and table S3, Materials and Methods). The primary model is shown to directly calculate δ at different site temperature (*T*, °C) and temperature change ranges (Δ*T*,°C) (fig. S6 and table S3). In (**B**), the red solid line shows the contemporary $Q_{10\,\overline{year},site}$ spatial patterns identical to the blue line in Fig. 1A, and the blue dashed lines are predictions of spatial $Q_{10\,\overline{year},site}$ patterns under different Representative Concentration Pathway scenarios (RCPs) until the end of the 21st century (2081–2100) based on the Coupled Model Intercomparison Project (CMIP5) (Materials and Methods). All site-scale predications are shown as dots in fig. S7 (F to I).

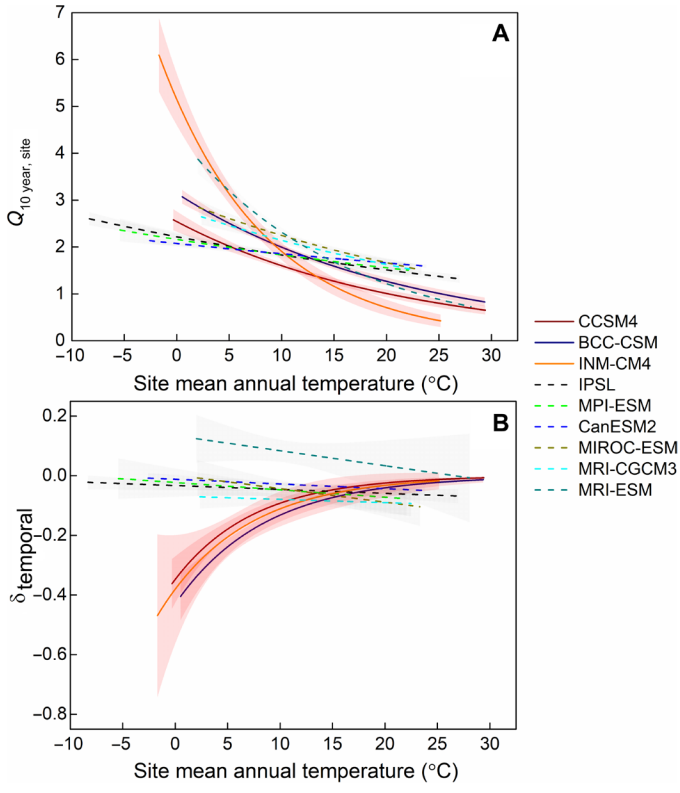

Fig. 4. Spatial patterns of Q_{10} and its temperature sensitivity against site mean annual temperature based on the nine model outputs from CMIP5 at the flux tower site. Solid curves represent those models considering the different temporal variations in $Q_{10\ year,\ site}$ under climate warming, while the dashed curves are not. The shadows are 95% confidence bands. Detailed regression and CMIP5 models' information are in the table S5, and the points are shown in fig. S10.

evidence for increasing limitations on substrate availability for decomposers as an important constraining factor (*25*, *26*). It is likely that multiple mechanisms work in tandem at varying strengths (*8*, *26*–*28*). In this study, the relationship between $Q_{10\,\overline{year},site}$ and $T_{\overline{year},site}$ was no longer significant when we grouped spatial sites with the same measured temperature ranges (Fig. 2, A to J, and fig. S3), suggesting that spatial variation in $Q_{10\,\overline{year},site}$ was likely caused by intrinsic factors such as the composition, quantity, and metabolic rates of microbes and plants, as well as inherent properties of enzymes under certain temperature levels (*23*, *29*–*31*). Moreover, the positive temperature-dependent trends observed in both $\delta_{temporal}$ and $\delta_{spatial}$ suggest that the temperature response of these intrinsic factors slowed with rising temperature. A meta-analysis of field warming experiments conducted during the past two decades (1994–2017), consistent with our result, also showed similar positive exponential temperature-dependent trends in $\delta_{temporal}$ (fig. S8, Materials and Methods). In addition, to test the compounding influences of the seasonal variability, especially the transition periods between growing season and non–growing season, we have reanalyzed our data after limiting to growing season for all sites. We also found that the results from these two methods showed similar trends in Q_{10} spatial-temporal variations (fig. S9), although the magnitude is different because of different available substrates (*25*, *26*) and temperature change ranges at different time scales.

Our findings, based on global field observational data, provide fresh insights on how the temperature sensitivity of Q_{10} has changed in recent time ($\delta_{temporal}$) and across space ($\delta_{spatial}$), as well as for the future warmer world. These results provide evidence for the potential convergence of global Q_{10} under ongoing climate warming, a warming response that is currently not reproduced by most Earth system models (six of nine CMIP5 models in Fig. 4 and fig. S10; Materials and Methods). Therefore, warming-induced carbon loss through *Re* at high-latitude regions may be less than assumptions in Earth system models because these projections underestimate the strong downward-adjustment of Q_{10} under climate warming, especially at

higher latitudes and in colder climates. Thus, this study calls for a careful reassessment of the predicted large carbon loss, especially at higher latitudes and in colder regions.

MATERIALS AND METHODS

EC-based data

For this study, we defined terrestrial ecosystem respiration (*Re*) as nighttime net CO_2 fluxes. The major dataset used in this study was the database of EC observations from a worldwide network of FLUXNET sites (*32*). All available half-hourly CO_2 flux and meteorological data from the FLUXNET (https://fluxnet.org/) were gathered, but sites with less than 5 years' data were excluded (called Data Set 0 comprising 929 site-years of 113 sites). Gap-filled data were excluded from the selected dataset to avoid spurious effects, and conventional quality control criteria were previously applied to the standard data files (*27*, *33*). If more than 25% of 1-year data or if continuous observations for more than 1 month were missing from a site, that particular site-year was excluded from the analysis completely. If less than five such full years of data were available for a site, we also excluded that site from the analysis. This data filtering was to ensure the continuity and reliability of the data used for further analyses. Air temperature data were extracted from the same databases to match the corresponding time of *Re* data. Here, we used air temperature (*T*) rather than soil temperature because both soil and vegetation respiration in *Re* responded to temperature (*34*).

Q_{10} calculation

Results from the statistical analysis (as following the "Statistical analysis" section) showed that temperature dominated seasonal variation of ecosystem respiration (table S1). Several models have been proposed to describe the temperature dependence of respiration (*35*, *36*). Here, we used a Q_{10}-based model (*37*) (S1), which describes the proportional increase in the rate of respiration per 10°C rise in temperature (*38*), derived from the Van't Hoff exponential chemical reaction–temperature equation (*39*)

$$Re = a \times e^{b \times T} \quad \text{(S1)}$$

where *Re* and *T* are half-hour nighttime (local time is later than 20 and earlier than 8) net CO_2 fluxes (ecosystem respiration) and corresponding air temperature in a particular year, respectively. *a* and *b* are the regression parameters that can be used to estimate Q_{10} values in a particular site-year from the following formula (*37*, *40*).

$$Q_{10\,\mathrm{year,site}} = e^{10 \times b} \quad \text{(S2)}$$

However, recent studies have also revealed that variation in temperature accounts for most of the variation in respiration in a particular site only in the absence of water stress (*38*, *41*). In other words, soil water content or precipitation deficits may also affect the temperature dependence of terrestrial respiration (*17*, *42*–*44*) and can even be the main controlling factor of terrestrial respiration under drier conditions (*45*, *46*). Therefore, we chose only sites for which the Van't Hoff equation showed a significant fit to the data ($P < 0.05$), which ensured that the influences from other factors (e.g., moisture or artificial management) on respiration were small in comparison to that of temperature. Last, 74 sites were extracted from Data Set 0 (called Data Set 1) and used to estimate the temperature sensitivity for a particular site-year ($Q_{10\ \mathrm{year,\ site}}$) (604 site-years in total; see table S1). All available nighttime respiration data from within a single year were used to estimate $Q_{10\ \mathrm{year,\ site}}$. The arithmetic means of annual $Q_{10\ \mathrm{year,\ site}}$ and $T_{\mathrm{year,\ site}}$ were used to estimate the spatial pattern of Q_{10} ($Q_{10\ \overline{\mathrm{year}},\mathrm{site}}$).

Furthermore, to inspect water restrictions, we tested the relationship between $Q_{10\ \mathrm{year,\ site}}$ and $T_{\mathrm{year,\ site}}$ when binned according to the annual drought index ($\mathrm{Dr}_{\mathrm{year,site}}$), the ratio of annual evapotranspiration ($\mathrm{ET}_{\mathrm{year,site}}$), and annual precipitation ($\mathrm{PPT}_{\mathrm{year,\ site}}$). Also, we tested the relationship between $Q_{10\ \mathrm{year,\ site}}$ and $\mathrm{Dr}_{\mathrm{year,site}}$ when binned by $T_{\mathrm{year,\ site}}$. The relationship between $Q_{10\ \mathrm{year,\ site}}$ and $T_{\mathrm{year,\ site}}$ are significant in all $\mathrm{Dr}_{\mathrm{year,site}}$ groups (fig. S1A). However, we did not find any significant relationship between $Q_{10\ \mathrm{year,\ site}}$ and $\mathrm{Dr}_{\mathrm{year,site}}$ (fig. S1B). In other words, the $\mathrm{Dr}_{\mathrm{year,site}}$ did not change the response of $Q_{10\ \mathrm{year,\ site}}$ to temperature despite the fact that a small number of site-years (15.6% of all site-years) have a higher $\mathrm{Dr}_{\mathrm{year,site}}$ (>1) (red line in fig. S1A). Thus, in this study, we focused on revealing the temperature effect on Q_{10}. Here, we did not use the soil water content because of the large amount of missing data and the inconsistent depth of field observations across the globe.

Temperature sensitivity of Q_{10} (δ)

We defined a new parameter δ, the rate of Q_{10} change per 1°C increase in mean annual temperature. This parameter is equivalent to the slope of the simple linear regression between $Q_{10\ \mathrm{year,\ site}}$ and $T_{\mathrm{year,\ site}}$ from long-term (>5 years per site) EC observational data (S3).

$$Q_{10\,\mathrm{year,site}} = \delta_{\mathrm{temporal}} \times T_{\mathrm{year,site}} + \varepsilon_{\mathrm{site}} \quad \text{(S3)}$$

where $\delta_{\mathrm{temporal}}$ represents the temporal temperature sensitivity of Q_{10} for an individual site. $Q_{10\ \mathrm{year,\ site}}$ is estimated for all available years at individual sites based on Eqs. S1 and S2 , $T_{\mathrm{year,\ site}}$ is the annual mean temperature, and $\varepsilon_{\mathrm{site}}$ is a site-specific regression parameter as the $Q_{10\ \mathrm{year,\ site}}$ when the $T_{\mathrm{year,\ site}}$ is 0°C.

However, this data-driven approach does not allow the determination of $\delta_{\mathrm{temporal}}$ under future global warming conditions, because the current-day temperature ranges at the sites typically do not fully encompass the projected future temperature ranges (*47*). To overcome this issue, space-for-time substitution provides an alternative, widely used approach to hindcast past and forecast future trajectories of ecosystem from the contemporary spatial patterns (*8*, *48*, *49*). However, the validity of this space-for-time substitution under future climate scenarios requires verification (*8*). Therefore, we also calculated the change rate of Q_{10} per 1°C change in temperature across the spatial gradient. Like $\delta_{\mathrm{temporal}}$, we designated the spatial temperature sensitivity of Q_{10} ($\delta_{\mathrm{spatial}}$). By definition, $\delta_{\mathrm{spatial}}$ can be calculated as the first derivative of the exponential, across-site relationship between $Q_{10\,\overline{\mathrm{year}},\mathrm{site}}$ and $T_{\overline{\mathrm{year}},\mathrm{site}}$ at each site-specific annual mean temperature (Eq. S4 and Fig. 1A).

$$\delta_{\mathrm{spatial}} = \frac{dQ_{10\overline{\mathrm{year}},\mathrm{site}}}{dT_{\overline{\mathrm{year}},\mathrm{site}}} \quad \text{(S4)}$$

Here, we did not apply a linear regression as was done for $\delta_{\mathrm{temporal}}$ because the spatial temperature change range was much larger than the within-site interannual temperature fluctuations. This, combined with the much larger number of data, revealed a better fit to the data when applying an exponential relation. Therefore, we chose to use the first derivative values to estimate $\delta_{\mathrm{spatial}}$.

Q_{10} estimates in STRs

We used STR Q_{10} estimates to test whether the difference between the spatial and temporal Q_{10} variations was explained solely by the differences in temperature or possibly attributable to geographical factors. First, we investigated a common temperature range that covered as many site-years in Data Set 1 as possible. After analyzing the annual mean temperature and the maximum and minimum temperatures of the 74 sites, we found a common temperature range (4° to 23°C) across all site-years (about 90% of all site-years) (fig. S2). Second, we created 10 groups of STRs from 4° to 23°C using a 10°C moving window to calculate Q_{10} values in each specific temperature bin [$Q_{10,\mathrm{str}(i\text{-}j)}$, $4°C \le i, j \le 23°C$] based on all available years' date at individual sites. The algorithm for calculating $Q_{10,\mathrm{str}(i\text{-}j)}$ is identical to the conventional Q_{10} calculation method (Eqs. S1 and S2). Here, we selected 10°C for the moving window in the estimation of $Q_{10,\mathrm{str}(i\text{-}j)}$ because by definition, Q_{10} is the proportional change in *Re* per 10°C rise in temperature. This way, we ensured comparability with most of the other sensitivity analyses of ecosystem respiration. In addition, to incorporate the likely effects of temperature moving windows on $Q_{10,\mathrm{str}(i\text{-}j)}$ variation, we also selected a series of temperature moving windows with the same mean measurement temperature to estimate $Q_{10,\mathrm{str}(i\text{-}j)}$ (fig. S3). Third, we investigated the relationships between $Q_{10,\mathrm{str}(i\text{-}j)}$ and site mean temperature in different temperature windows across all site-years (Fig. 2, A to J). Moreover, $Q_{10,\mathrm{str}(i\text{-}j)}$ values were respectively aggregated by their arithmetic mean ($Q_{10,\overline{\mathrm{str}(i\text{-}j)}}$) in different temperature ranges and temperature moving windows (Fig. 2 and fig. S3). Last, we tested the differences of mean $Q_{10,\overline{\mathrm{str}(i\text{-}j)}}$ at the same mean measurement temperature among these series of temperature moving windows (fig. S3).

Comparison of $\delta_{temporal}$ and $\delta_{spatial}$ across different temperature change gradients

The fact that $\delta_{spatial}$ was calculated from a large temperature variation (about 25°C in our Data Set 1), while $\delta_{temporal}$ only over a much smaller interannual range in mean annual temperature (generally 1° to 3°C) (Fig. 1A), reduces the comparability of both indicators for the temperature dependence of Q_{10}. Therefore, we want to test the agreement between $\delta_{spatial}$ and $\delta_{temporal}$ at both the same temperature and temperature change range. First, we calculated the spatial patterns of $Q_{10\,\overline{year},site}$ for temperature change ranges using moving windows from 25°, 20°, and down to 2°C (by 1°C steps, 20 groups in total). As the spatial temperature gradient across all sites is about 25°C in Data Set 1, we extracted multiple exponential spatial patterns of $Q_{10\,\overline{year},site}$ along each moving temperature gradient window from 24° to 2°C. For example, for a moving window of 20°C, we derived the exponential spatial patterns of $Q_{10\,\overline{year},site}$ against site temperature changes from −5° to 15°C, but also from 0° to 20°C (dots in Fig. 1A). All these patterns were included to ensure robust results across the globe.

Second, using Eq. S4, we calculated $\delta_{spatial}$ values across different spatial temperature change windows from 25° to 2°C, respectively (black dots in fig. S4). The optimal exponential curves of these $\delta_{spatial}$ values were designated as $\delta_{spatial,\ specific\ temperature\ windows}$ (e.g., $\delta_{spatial,\ 20°C}$ and $\delta_{spatial,\ 2°C}$) (red lines in fig. S4 and table S3). However, the spatial pattern of $Q_{10\,\overline{year},site}$ across 1°C temperature windows showed a great variation, and it was very difficult to obtain a robust value of $\delta_{spatial,\ 1°C}$. Furthermore, we grouped the $\delta_{temporal}$ of all observational sites according to the interannual temperature changes, the difference between the maximum and minimum annual mean temperature of one site, into approximately 1°C (0.5° to 1.5°C; blue dots in fig. S5), 2°C (1.5° to 2.5°C; red dots in fig. S4T), and 3°C (2.5° to 3.5°C; red dots in fig. S4S), respectively. Last, we inspected the agreement between $\delta_{spatial}$ and $\delta_{temporal}$ across similar temperature change window from 2° to 3°C, respectively. If the space-for-time substitution is valid (i.e., it does not show a significant difference between $\delta_{spatial}$ and $\delta_{temporal}$), then it would imply that we can use the $\delta_{spatial}$ across different temperature gradients to predict temporal variations of Q_{10} under climate warming.

Q_{10} prediction under climate warming

On the basis of contemporary spatial $Q_{10\,\overline{year},site}$ pattern (Fig. 1A) and site-specific $\delta_{temporal}$ values, we can directly predict a global spatial $Q_{10\,\overline{year},site}$ pattern under ongoing 1°C equilibrium warming scenario (Eq. S5). However, only quantifying global $Q_{10\,\overline{year},site}$ pattern under a 1°C warming scenario is not explicit enough to illuminate the further $Q_{10\,\overline{year},site}$ patterns under the projected climate warming (*50*, *51*). Thus, we further examined what the global spatial $Q_{10\,\overline{year},site}$ pattern would be under future warming scenarios in 1°C steps based on the $\delta_{spatial,\ i\,°C}$ derived from space-for-time substitution (Eq. S5)

$$Q_{10\overline{year},site,+i°C} = Q_{10\overline{year},site,+(i\text{-}1)\,°C} + \begin{cases} \delta_{temporal}(i = 1) \\ \delta_{spatial,i°C}(i > 1) \end{cases} (i = 1,2,\ldots,n, n \in Z^{+}) \quad \text{(S5)}$$

where i is the projected warming scenario, and $Q_{10\overline{year},site,+i\,°C}$ is the projected spatial $Q_{10\,\overline{year},site}$ under the i °C warming scenario. Here, $\delta_{temporal}$ is the temporal temperature sensitivity of $Q_{10\ year,\ site}$, and $\delta_{spatial,\ i\,°C}$ is the spatial temperature sensitivity of $Q_{10\,\overline{year},site}$ with an i °C temperature change window. For example, if one site, with T °C site temperature, is projected to have a 3°C warming scenario ($i = 3$) and current Q_{10} is $Q_{10\,\overline{year},site}$, then we will use the next three steps to estimate the $Q_{10\,\overline{year},site}$ variation: (i) We need to calculate the $\delta_{temporal}$ of this site (T °C temperature inputs, $\delta_{temporal,\ site}$) according to $\delta_{temporal}$ variation against site temperature (Fig. 1B and table S3). The sum of $\delta_{temporal,\ site}$ and $Q_{10\,\overline{year},site}$ is the Q_{10} estimation of this site under 1°C warming scenario ($Q_{10\overline{year},site,+1\,°C}$). (ii) Similar to the first step, we need to check the $\delta_{spatial,\ 2°C}$ variation against site temperature to estimate $\delta_{spatial}$ at this site (note here T + 1°C temperature inputs, $\delta_{spatial,\ 2°C,\ site}$) (table S3). The sum of $Q_{10\overline{year},site,+1\,°C}$ and $\delta_{spatial,\ 2°C,\ site}$ is the Q_{10} estimation of this site under 2°C warming scenario ($Q_{10\overline{year},site,+2\,°C}$). (iii) In the same way, we can calculate $\delta_{spatial,\ 3°C,\ site}$ at T + 2°C temperature inputs and $Q_{10\overline{year},site,+3\,°C}$ for this site under 3°C warming scenario. In addition, we also provided a general model for parameters of δ patterns (a and b in $\delta = a \times e^{b \times T}$) at different temperature change ranges (Fig. 3A, table S3, and fig. S6). Together with Eq. S5, we can directly estimate Q_{10} variation response to warming for a certain site.

In this study, we used two kinds of warming scenarios to describe future $Q_{10\,\overline{year},site}$ patterns. One was the spatial equilibrium warming scenario by 1°C warming step, which provided an intuitive result in how $Q_{10\,\overline{year},site}$ is likely to change under future warming conditions from 1° to 5°C (fig. S7, A to E). The other was the site-specific warming scenario, a nonequal warming trend across sites, evaluated by the CMIP5 under all RCP scenarios (2.6, 4.5, 6.0, and 8.5) until the end of the 21st century (2081–2100) based on the Intergovernmental Panel on Climate Change (IPCC) Fifth Assessment Report (*50*) (fig.

S7, F to I, and table S2). The method of $Q_{10\,\overline{year},site}$ projections is identical to the spatial-equilibrium warming scenario, as Eq. S5 shows.

Statistical analysis

To explore the main driving factors of seasonal Re, we developed correlation analysis (COR) and partial correlation analysis (PCOR) between ecosystem respiration (Re) and climate factors at a particular site-year, including temperature (T), vapor pressure deficit (VPD; considering the data missing, VPD could be replaced by soil water content or relative humidity), and PPT (table S1). Both COR (table S1) and PCOR (similar to COR, thus are not included here) showed a greater correlation of temperature at most sites (68 of 72 sites, the remaining 2 sites do not have enough VPD data for COR and PCOR), which indicated that temperature dominated the seasonal variation of ecosystem respiration, not VPD or PPT. To examine the role of ecosystem types or climatic regions in determining the patterns of $Q_{10\,\overline{year},site}$ and δ, we grouped all sites into different components using two schemes. One classified sites by ecosystem types, including croplands (CRO), forests [FOR; including evergreen needle leaf forests (ENF), evergreen broadleaf forests (EBF), mixed deciduous and evergreen forests (MF), and deciduous broadleaf forests (DBF)], shrubs [SHR; including closed shrublands (CSH), open shrub (OSH), and woody savannas (WSA)], grasslands (GRA), and wetlands (WET) (table S1). The other classification grouped sites into three climatic regions: arctic and boreal, temperate, and (sub-)tropical (table S2). These data passed the normality test (Shapiro-Wilk test) and homogeneity of variance test (Bartlett test) ($P > 0.05$). Next, we used a one-way analysis of variance and Tukey's post hoc to test for multiple comparisons across different climate biomes or among different ecosystem types to investigate the spatial variability of $Q_{10\,\overline{year},site}$ (δ) at $\alpha = 0.05$ (table S2). From the results given in table S2, we discovered that only the climatic regions, not the ecosystem types, showed significant $Q_{10\,\overline{year},site}$ (and δ) spatial differences. Therefore, we can ignore the small confounding effects of ecosystem types on $Q_{10\,\overline{year},site}$ (and δ) spatial variation with temperature fluctuations in our next analysis (*52*). In addition, we tested the differences between the $\delta_{temporal}$ and $\delta_{spatial}$ using paired t test at $\alpha = 0.05$ among the groups as mentioned above. All statistical and modeling procedures were performed using the R statistical computing packages (Version 3.5.0) (www.r-project.org).

Meta-analysis

We searched peer-reviewed journal articles including "experimental warming, temperature sensitivity (Q_{10}), ecosystem respiration, or soil respiration" using Web of Science in the past two decades (1994–2017). Then, we only selected the studies that (i) manipulated warming in the field, (ii) had clear control and experimental groups, (iii) had calculated Q_{10} for two groups or for which it could be calculated from complete observations of respiration and temperature, and (iv) included at least one whole growing season. Last, we extracted 54 field warming studies across the globe in our meta-analysis (table S4). We synthesized the Q_{10} values and temperature measurements for the experimental group (warming: $Q_{10,\,W}$ and T_W) and the control group (nonwarming: $Q_{10,\,C}$ and T_C) at individual sites. Using the similar method with EC-based $\delta_{temporal}$ calculation (Eq. S3), we also calculated the $\delta_{temporal}$ based on these data from field-warming experiments (WE-based $\delta_{temporal}$) (Eq. S6).

$$\delta_{temporal} = \frac{Q_{10,W} - Q_{10,C}}{T_W - T_C} \quad \text{(S6)}$$

Then, we compared the WE-based $\delta_{temporal}$ with EC-based $\delta_{temporal}$ along a similar temperature gradient.

CMIP5 models comparison

Using the 74 flux tower positions (table S1) as the center pixel, we extracted nine model outputs, including autotrophic respiration (Ra), heterotrophic respiration (Rh), and temperature, from CMIP5 to estimate their $Q_{10\,year,\,site}$ and trend in time ($\delta_{temporal}$) over two decades (1990–2012). The detailed model information is shown in the table S5, and the estimation methods of $Q_{10\,year,\,site}$ and $\delta_{temporal}$ are identical to Eqs. S1 to S3 , in which the Re was regarded as the sum of Ra and Rh. Overall, this analysis showed that most Earth system models (six of nine, in this study) ignored variation of $\delta_{temporal}$ under climate warming despite considering the spatial variation of $Q_{10\,\overline{year},site}$, except for CCSM4, BCC-CSM, and INM-CM4, whose temporal trends of $Q_{10\,year,\,site}$ across sites were similar to the EC-based result (Figs. 1B and 4 and fig. S10). Thus, although Q_{10} input in these models is typically insensitive to temperature and generally well approximated ($Q_{10} = 2$) according to specific documentations, some Earth system models also take into account the temperature-dependent Q_{10} using some specific functions and parameters. For example, the Carbon Exchange between Vegetation, Soil, and Atmosphere (CEVSA) model in the BCC-CSM introduced a temperature-dependent piecewise function to adjust the Q_{10} inputs (*53*–*55*). Our results suggested that a series of temperature-dependent decline rate in Q_{10} ($\delta_{temporal}$) across the globe respond to different climate warming scenarios (Fig. 3 and table S3), which can be applicable to adjust the Q_{10} inputs for many Earth system models in future carbon efflux estimation. However, future warming may enhance water stress in arid regions, which is likely to affect the climate-carbon feedback with more complex situations and make it more difficult to extrapolate to future climates (*56*). Therefore, future continuous water scaling researches, especially in the arid and semiarid regions, are still needed for an adequate mechanism explanation in carbon-climate feedback.

SUPPLEMENTARY MATERIALS

Supplementary material for this article is available at http://advances.sciencemag.org/cgi/content/full/7/15/eabc7358/DC1

REFERENCES AND NOTES

1. P. Friedlingstein, M. Meinshausen, V. K. Arora, C. D. Jones, A. Anav, S. K. Liddicoat, R. Knutti, Uncertainties in CMIP5 climate projections due to carbon cycle feedbacks. *J. Clim.* **27**, 511–526 (2014).
2. Y. Luo, S. Wan, D. Hui, L. L. Wallace, Acclimatization of soil respiration to warming in a tall grass prairie. *Nature* **413**, 622–625 (2001).
3. M. U. F. Kirschbaum, The temperature dependence of organic-matter decomposition––still a topic of debate. *Soil Biol. Biochem.* **38**, 2510–2518 (2006).
4. W. Knorr, I. C. Prentice, J. I. House, E. A. Holland, Long-term sensitivity of soil carbon turnover to warming. *Nature* **433**, 298–301 (2005).
5. B. Bond-Lamberty, A. Thomson, Temperature-associated increases in the global soil respiration record. *Nature* **464**, 579–582 (2010).
6. C. Huntingford, O. K. Atkin, A. Martinez-de la Torre, L. M. Mercado, M. A. Heskel, A. B. Harper, K. J. Bloomfield, O. S. O'Sullivan, P. B. Reich, K. R. Wythers, E. E. Butler, M. Chen, K. L. Griffin, P. Meir, M. G. Tjoelker, M. H. Turnbull, S. Sitch, A. Wiltshire, Y. Malhi, Implications of improved representations of plant respiration in a changing climate. *Nat. Commun.* **8**, 1602 (2017).
7. N. G. Smith, J. S. Dukes, Plant respiration and photosynthesis in global-scale models: Incorporating acclimation to temperature and CO_2. *Glob. Chang. Biol.* **19**, 45–63 (2013).

8. E. A. Davidson, I. A. Janssens, Temperature sensitivity of soil carbon decomposition and feedbacks to climate change. *Nature* **440**, 165–173 (2006).
9. P. M. Cox, D. Pearson, B. B. Booth, P. Friedlingstein, C. Huntingford, C. D. Jones, C. M. Luke, Sensitivity of tropical carbon to climate change constrained by carbon dioxide variability. *Nature* **494**, 341–344 (2013).
10. I. Ilie, P. Dittrich, N. Carvalhais, M. Jung, A. Heinemeyer, M. Migliavacca, J. I. L. Morison, S. Sippel, J. A. Subke, M. Wilkinson, M. D. Mahecha, Reverse engineering model structures for soil and ecosystem respiration: The potential of gene expression programming. *Geosci. Model Dev.* **10**, 3519–3545 (2017).
11. C. D. Koven, G. Hugelius, D. M. Lawrence, W. R. Wieder, Higher climatological temperature sensitivity of soil carbon in cold than warm climates. *Nat. Clim. Chang.* **7**, 817–822 (2017).
12. M. Reichstein, C. Beer, Soil respiration across scales: The importance of a model–data integration framework for data interpretation. *J. Plant Nutr. Soil Sci.* **171**, 344–354 (2008).
13. P. M. Cox, R. A. Betts, C. D. Jones, S. A. Spall, I. J. Totterdell, Acceleration of global warming due to carbon-cycle feedbacks in a coupled climate model. *Nature* **408**, 184–187 (2000).
14. S. Hamdi, F. Moyano, S. Sall, M. Bernoux, T. Chevallier, Synthesis analysis of the temperature sensitivity of soil respiration from laboratory studies in relation to incubation methods and soil conditions. *Soil Biol. Biochem.* **58**, 115–126 (2013).
15. N. G. Smith, S. L. Malyshev, E. Shevliakova, J. Kattge, J. S. Dukes, Foliar temperature acclimation reduces simulated carbon sensitivity to climate. *Nat. Clim. Chang.* **6**, 407–411 (2016).
16. N. Meyer, G. Welp, W. Amelung, The temperature sensitivity (Q10) of soil respiration: Controlling factors and spatial prediction at regional scale based on environmental soil classes. *Glob. Biogeochem. Cycles* **32**, 306–323 (2018).
17. S. S. Peng, S. L. Piao, T. Wang, J. Y. Sun, Z. H. Shen, Temperature sensitivity of soil respiration in different ecosystems in China. *Soil Biol. Biochem.* **41**, 1008–1014 (2009).
18. T. W. Crowther, K. E. O. Todd-Brown, C. W. Rowe, W. R. Wieder, J. C. Carey, M. B. Machmuller, B. L. Snoek, S. Fang, G. Zhou, S. D. Allison, J. M. Blair, S. D. Bridgham, A. J. Burton, Y. Carrillo, P. B. Reich, J. S. Clark, A. T. Classen, F. A. Dijkstra, B. Elberling, B. A. Emmett, M. Estiarte, S. D. Frey, J. Guo, J. Harte, L. Jiang, B. R. Johnson, G. Kröel-Dulay, K. S. Larsen, H. Laudon, J. M. Lavallee, Y. Luo, M. Lupascu, L. N. Ma, S. Marhan, A. Michelsen, J. Mohan, S. Niu, E. Pendall, J. Peñuelas, L. Pfeifer-Meister, C. Poll, S. Reinsch, L. L. Reynolds, I. K. Schmidt, S. Sistla, N. W. Sokol, P. H. Templer, K. K. Treseder, J. M. Welker, M. A. Bradford, Quantifying global soil carbon losses in response to warming. *Nature* **540**, 104–108 (2016).
19. H. J. De Boeck, S. Vicca, J. Roy, I. Nijs, A. Milcu, J. Kreyling, A. Jentsch, A. Chabbi, M. Campioli, T. Callaghan, C. Beierkuhnlein, C. Beier, Global change experiments: Challenges and opportunities. *Bioscience* **65**, 922–931 (2015).
20. C. E. Smyth, W. A. Kurz, Forest soil decomposition and its contribution to heterotrophic respiration: A case study based on Canada. *Soil Biol. Biochem.* **67**, 155–165 (2013).
21. T. Stocker, D. Qin, G.-K. Plattner, M. M. B. Tignor, S. K. Allen, J. Boschung, A. Nauels, Y. Xia, V. Bex, P. M. Midgley, Climate change 2013: The physical science basis. Contribution of working group I to the fifth assessment report of the intergovernmental panel on climate change (2013).
22. M. A. Bradford, C. A. Davies, S. D. Frey, T. R. Maddox, J. M. Melillo, J. E. Mohan, J. F. Reynolds, K. K. Treseder, M. D. Wallenstein, Thermal adaptation of soil microbial respiration to elevated temperature. *Ecol. Lett.* **11**, 1316–1327 (2008).
23. O. K. Atkin, M. G. Tjoelker, Thermal acclimation and the dynamic response of plant respiration to temperature. *Trends Plant Sci.* **8**, 343–351 (2003).
24. S. Niu, Y. Luo, S. Fei, W. Yuan, D. Schimel, B. E. Law, C. Ammann, M. Altaf Arain, A. Arneth, M. Aubinet, A. Barr, J. Beringer, C. Bernhofer, T. Andrew Black, N. Buchmann, A. Cescatti, J. Chen, K. J. Davis, E. Dellwik, A. R. Desai, S. Etzold, L. Francois, D. Gianelle, B. Gielen, A. Goldstein, M. Groenendijk, L. Gu, N. Hanan, C. Helfter, T. Hirano, D. Y. Hollinger, M. B. Jones, G. Kiely, T. E. Kolb, W. L. Kutsch, P. Lafleur, D. M. Lawrence, L. Li, A. Lindroth, M. Litvak, D. Loustau, M. Lund, M. Marek, T. A. Martin, G. Matteucci, M. Migliavacca, L. Montagnani, E. Moors, J. William Munger, A. Noormets, W. Oechel, J. Olejnik, K. T. P. U, K. Pilegaard, S. Rambal, A. Raschi, R. L. Scott, G. Seufert, D. Spano, P. Stoy, M. A. Sutton, A. Varlagin, T. Vesala, E. Weng, G. Wohlfahrt, B. Yang, Z. Zhang, X. Zhou, Thermal optimality of net ecosystem exchange of carbon dioxide and underlying mechanisms. *New Phytol.* **194**, 775–783 (2012).
25. I. P. Hartley, D. W. Hopkins, M. H. Garnett, M. Sommerkorn, P. A. Wookey, No evidence for compensatory thermal adaptation of soil microbial respiration in the study of Bradford et al. (2008). *Ecol. Lett.* **12**, E12–E14 (2009).
26. G. I. Ågren, J. Å. M. Wetterstedt, What determines the temperature response of soil organic matter decomposition? *Soil Biol. Biochem.* **39**, 1794–1798 (2007).
27. M. D. Mahecha, M. Reichstein, N. Carvalhais, G. Lasslop, H. Lange, S. I. Seneviratne, R. Vargas, C. Ammann, M. A. Arain, A. Cescatti, I. A. Janssens, M. Migliavacca, L. Montagnani, A. D. Richardson, Global convergence in the temperature sensitivity of respiration at ecosystem level. *Science* **329**, 838–840 (2010).
28. J. M. Melillo, S. D. Frey, K. M. DeAngelis, W. J. Werner, M. J. Bernard, F. P. Bowles, G. Pold, M. A. Knorr, A. S. Grandy, Long-term pattern and magnitude of soil carbon feedback to the climate system in a warming world. *Science* **358**, 101–105 (2017).
29. K. Karhu, M. D. Auffret, J. A. J. Dungait, D. W. Hopkins, J. I. Prosser, B. K. Singh, J.-A. Subke, P. A. Wookey, G. I. Ågren, M.-T. Sebastià, F. Gouriveau, G. Bergkvist, P. Meir, A. T. Nottingham, N. Salinas, I. P. Hartley, Temperature sensitivity of soil respiration rates enhanced by microbial community response. *Nature* **513**, 81–84 (2014).
30. S. D. Frey, J. Lee, J. M. Melillo, J. Six, The temperature response of soil microbial efficiency and its feedback to climate. *Nat. Clim. Chang.* **3**, 395–398 (2013).
31. M. A. Heskel, O. S. O'Sullivan, P. B. Reich, M. G. Tjoelker, L. K. Weerasinghe, A. Penillard, J. J. G. Egerton, D. Creek, K. J. Bloomfield, J. Xiang, F. Sinca, Z. R. Stangl, A. Martinez-de la Torre, K. L. Griffin, C. Huntingford, V. Hurry, P. Meir, M. H. Turnbull, O. K. Atkin, Convergence in the temperature response of leaf respiration across biomes and plant functional types. *Proc. Natl. Acad. Sci. U.S.A.* **113**, 3832–3837 (2016).
32. D. Baldocchi, E. Falge, L. Gu, R. Olson, D. Hollinger, S. Running, P. Anthoni, C. Bernhofer, K. Davis, R. Evans, J. Fuentes, A. Goldstein, G. Katul, B. Law, X. Lee, Y. Malhi, T. Meyers, W. Munger, W. Oechel, K. T. Paw, K. Pilegaard, H. P. Schmid, R. Valentini, S. Verma, T. Vesala, K. Wilson, S. Wofsy, FLUXNET: A new tool to study the temporal and spatial variability of ecosystem-scale carbon dioxide, water vapor, and energy flux densities. *Bull. Am. Meteorol. Soc.* **82**, 2415–2434 (2001).
33. D. Papale, M. Reichstein, M. Aubinet, E. Canfora, C. Bernhofer, W. Kutsch, B. Longdoz, S. Rambal, R. Valentini, T. Vesala, D. Yakir, Towards a standardized processing of net ecosystem exchange measured with eddy covariance technique: Algorithms and uncertainty estimation. *Biogeosciences* **3**, 571–583 (2006).
34. M. D. Mahecha, M. Reichstein, N. Carvalhais, G. Lasslop, H. Lange, S. I. Seneviratne, R. Vargas, C. Ammann, M. A. Arain, A. Cescatti, I. A. Janssens, M. Migliavacca, L. Montagnani, A. D. Richardson, Response to comment on "Global Convergence in the Temperature Sensitivity of Respiration at Ecosystem Level". *Science* **331**, 1265 (2011).
35. D. M. Perkins, G. Yvon-Durocher, B. O. L. Demars, J. Reiss, D. E. Pichler, N. Friberg, M. Trimmer, G. Woodward, Consistent temperature dependence of respiration across ecosystems contrasting in thermal history. *Glob. Chang. Biol.* **18**, 1300–1311 (2012).
36. M. Tuomi, P. Vanhala, K. Karhu, H. Fritze, J. Liski, Heterotrophic soil respiration–– Comparison of different models describing its temperature dependence. *Ecol. Model.* **211**, 182–190 (2008).
37. J. Lloyd, J. A. Taylor, On the temperature-dependence of soil respiration. *Funct. Ecol.* **8**, 315–323 (1994).
38. E. A. Davidson, E. Belk, R. D. Boone, Soil water content and temperature as independent or confounded factors controlling soil respiration in a temperate mixed hardwood forest. *Glob. Chang. Biol.* **4**, 217–227 (1998).
39. J. H. van't Hoff, Über die zunehmende Bedeutung der anorganischen Chemie. Vortrag, gehalten auf der 70. Versammlung der Gesellschaft deutscher Naturforscher und Ärzte zu Düsseldorf. *Z. Anorg. Chem.* **18**, 1–13 (1898).
40. J. W. Raich, W. H. Schlesinger, The global carbon-dioxide flux in soil respiration and its relationship to vegetation and climate. *Tellus Ser. B Chem. Phys. Meteorol.* **44**, 81–99 (1992).
41. M. Xu, Y. Qi, Spatial and seasonal variations of Q_{10} determined by soil respiration measurements at a Sierra Nevadan Forest. *Glob. Biogeochem. Cycles* **15**, 687–696 (2001).
42. B. Song, S. Niu, R. Luo, Y. Luo, J. Chen, G. Yu, J. Olejnik, G. Wohlfahrt, G. Kiely, A. Noormets, L. Montagnani, A. Cescatti, V. Magliulo, B. E. Law, M. Lund, A. Varlagin, A. Raschi, M. Peichl, M. B. Nilsson, L. Merbold, Divergent apparent temperature sensitivity of terrestrial ecosystem respiration. *J. Plant Ecol.* **7**, 419–428 (2014).
43. V. Suseela, R. T. Conant, M. D. Wallenstein, J. S. Dukes, Effects of soil moisture on the temperature sensitivity of heterotrophic respiration vary seasonally in an old-field climate change experiment. *Glob. Chang. Biol.* **18**, 336–348 (2012).
44. L. Xu, D. D. Baldocchi, J. Tang, How soil moisture, rain pulses, and growth alter the response of ecosystem respiration to temperature. *Glob. Biogeochem. Cycles* **18**, GB4002 (2004).
45. E. A. Davidson, I. A. Janssens, Y. Luo, On the variability of respiration in terrestrial ecosystems: Moving beyond Q_{10}. *Glob. Chang. Biol.* **12**, 154–164 (2006).
46. L. L. Reynolds, B. R. Johnson, L. Pfeifer-Meister, S. D. Bridgham, Soil respiration response to climate change in Pacific Northwest prairies is mediated by a regional Mediterranean climate gradient. *Glob. Chang. Biol.* **21**, 487–500 (2015).
47. Y. Q. Luo, Terrestrial carbon-cycle feedback to climate warming. *Annu. Rev. Ecol. Evol. Syst.* **38**, 683–712 (2007).
48. J. L. Blois, J. W. Williams, M. C. Fitzpatrick, S. T. Jackson, S. Ferrier, Space can substitute for time in predicting climate-change effects on biodiversity. *Proc. Natl. Acad. Sci. U.S.A.* **110**, 9374–9379 (2013).
49. M. G. Tjoelker, J. Oleksyn, P. B. Reich, Modelling respiration of vegetation: Evidence for a general temperature-dependent Q_{10}. *Glob. Chang. Biol.* **7**, 223–230 (2001).
50. IPCC, *Climate Change 2014–Impacts, Adaptation and Vulnerability: Regional Aspects* (Cambridge Univ. Press, 2014).

51. D. J. A. Johansson, B. C. O'Neill, C. Tebaldi, O. Häggström, Equilibrium climate sensitivity in light of observations over the warming hiatus. *Nat. Clim. Chang.* **5**, 449–453 (2015).
52. X. Wang, S. Piao, P. Ciais, I. A. Janssens, M. Reichstein, S. Peng, T. Wang, Are ecological gradients in seasonal Q_{10} of soil respiration explained by climate or by vegetation seasonality? *Soil Biol. Biochem.* **42**, 1728–1734 (2010).
53. M. Cao, F. I. Woodward, Dynamic responses of terrestrial ecosystem carbon cycling to global climate change. *Nature* **393**, 249–252 (1998).
54. F. I. Woodward, T. M. Smith, W. R. Emanuel, A global land primary productivity and phytogeography model. *Glob. Biogeochem. Cycles* **9**, 471–490 (1995).
55. M. Cao, F. I. Woodward, Net primary and ecosystem production and carbon stocks of terrestrial ecosystems and their responses to climate change. *Glob. Chang. Biol.* **4**, 185–198 (1998).
56. Q. Quan, D. Tian, Y. Luo, F. Zhang, T. W. Crowther, K. Zhu, H. Y. H. Chen, Q. Zhou, S. Niu, Water scaling of ecosystem carbon cycle feedback to climate warming. *Sci. Adv.* **5**, eaav1131 (2019).
57. E. van Gorsel, R. Leuning, H. A. Cleugh, H. Keith, M. U. F. Kirschbaum, T. Suni, Application of an alternative method to derive reliable estimates of nighttime respiration from eddy covariance measurements in moderately complex topography. *Agric. For. Meteorol.* **148**, 1174–1180 (2008).
58. M. Aubinet, B. Chermanne, M. Vandenhaute, B. Longdoz, M. Yernaux, E. Laitat, Long term carbon dioxide exchange above a mixed forest in the Belgian Ardennes. *Agric. For. Meteorol.* **108**, 293–315 (2001).
59. P. M. Lafleur, N. T. Roulet, J. L. Bubier, S. Frolking, T. R. Moore, Interannual variability in the peatland-atmosphere carbon dioxide exchange at an ombrotrophic bog. *Glob. Biogeochem. Cycles* **17**, 1036 (2003).
60. A. Knohl, E.-D. Schulze, O. Kolle, N. Buchmann, Large carbon uptake by an unmanaged 250-year-old deciduous forest in Central Germany. *Agric. For. Meteorol.* **118**, 151–167 (2003).
61. R. Valentini, G. Matteucci, A. J. Dolman, E. D. Schulze, C. Rebmann, E. J. Moors, A. Granier, P. Gross, N. O. Jensen, K. Pilegaard, A. Lindroth, A. Grelle, C. Bernhofer, T. Grünwald, M. Aubinet, R. Ceulemans, A. S. Kowalski, T. Vesala, Ü. Rannik, P. Berbigier, D. Loustau, J. Guðmundsson, H. Thorgeirsson, A. Ibrom, K. Morgenstern, R. Clement, J. Moncrieff, L. Montagnani, S. Minerbi, P. G. Jarvis, Respiration as the main determinant of carbon balance in European forests. *Nature* **404**, 861–865 (2000).
62. K. Pilegaard, K. Pilegaard, T. N. Mikkelsen, C. Beier, N. O. Jensen, P. L. Ambus, H. Ro-Poulsen, Field measurements of atmosphere-biosphere interactions in a Danish beech forest. *Boreal Environ. Res.* **8**, 315–333 (2003).
63. C. Rebmann, M. Göckede, T. Foken, M. Aubinet, M. Aurela, P. Berbigier, C. Bernhofer, N. Buchmann, A. Carrara, A. Cescatti, R. Ceulemans, R. Clement, J. A. Elbers, A. Granier, T. Grünwald, D. Guyon, K. Havránková, B. Heinesch, A. Knohl, T. Laurila, B. Longdoz, B. Marcolla, T. Markkanen, F. Miglietta, J. Moncrieff, L. Montagnani, E. Moors, M. Nardino, J. M. Ourcival, S. Rambal, Ü. Rannik, E. Rotenberg, P. Sedlak, G. Unterhuber, T. Vesala, D. Yakir, Quality analysis applied on eddy covariance measurements at complex forest sites using footprint modelling. *Theor. Appl. Climatol.* **80**, 121–141 (2005).
64. T. Suni, J. Rinne, A. Reissell, N. Altimir, P. Keronen, Ü. Rannik, M. D. Maso, M. Kulmala, T. Vesala, Long-term measurements of surface fluxes above a Scots pine forest in Hyytiälä, southern Finland, 1996-2001. *Boreal Environ. Res.* **8**, 287–301 (2003).
65. A. Granier, E. Ceschia, C. Damesin, E. Dufrêne, D. Epron, P. Gross, S. Lebaube, V. le Dantec, N. le Goff, D. Lemoine, E. Lucot, J. M. Ottorini, J. Y. Pontailler, B. Saugier, The carbon balance of a young Beech forest. *Funct. Ecol.* **14**, 312–325 (2000).
66. P. Berbigier, J.-M. Bonnefond, P. Mellmann, CO_2 and water vapour fluxes for 2 years above Euroflux forest site. *Agric. For. Meteorol.* **108**, 183–197 (2001).
67. S. Rambal, R. Joffre, J. M. Ourcival, J. Cavender-Bares, A. Rocheteau, The growth respiration component in eddy CO_2 flux from a *Quercus ilex* mediterranean forest. *Glob. Chang. Biol.* **10**, 1460–1469 (2004).
68. T. G. Gilmanov, J. F. Soussana, L. Aires, V. Allard, C. Ammann, M. Balzarolo, Z. Barcza, C. Bernhofer, C. L. Campbell, A. Cernusca, A. Cescatti, J. Clifton-Brown, B. O. M. Dirks, S. Dore, W. Eugster, J. Fuhrer, C. Gimeno, T. Gruenwald, L. Haszpra, A. Hensen, A. Ibrom, A. F. G. Jacobs, M. B. Jones, G. Lanigan, T. Laurila, A. Lohila, G. Manca, B. Marcolla, Z. Nagy, K. Pilegaard, K. Pinter, C. Pio, A. Raschi, N. Rogiers, M. J. Sanz, P. Stefani, M. Sutton, Z. Tuba, R. Valentini, M. L. Williams, G. Wohlfahrt, Partitioning European grassland net ecosystem CO_2 exchange into gross primary productivity and ecosystem respiration using light response function analysis. *Agric. Ecosyst. Environ.* **121**, 93–120 (2007).
69. A. I. J. M. Van Dijk, A. J. Dolman, Estimates of CO_2 uptake and release among European forests based on eddy covariance data. *Glob. Chang. Biol.* **10**, 1445–1459 (2004).
70. M. F. Garbulsky, J. Penuelas, D. Papale, I. Filella, Remote estimation of carbon dioxide uptake by a Mediterranean forest. *Glob. Chang. Biol.* **14**, 2860–2867 (2008).
71. A. Rey, E. Pegoraro, V. Tedeschi, I. de Parri, P. G. Jarvis, R. Valentini, Annual variation in soil respiration and its components in a coppice oak forest in Central Italy. *Glob. Chang. Biol.* **8**, 851–866 (2002).
72. V. Tedeschi, A. Rey, G. Manca, R. Valentini, P. G. Jarvis, M. Borghetti, Soil respiration in a Mediterranean oak forest at different developmental stages after coppicing. *Glob. Chang. Biol.* **12**, 110–121 (2006).
73. M. Chiesi, F. Maselli, M. Bindi, L. Fibbi, P. Cherubini, E. Arlotta, G. Tirone, G. Matteucci, G. Seufert, Modelling carbon budget of Mediterranean forests using ground and remote sensing measurements. *Agric. For. Meteorol.* **135**, 22–34 (2005).
74. A. J. Dolman, E. J. Moors, J. A. Elbers, The carbon uptake of a mid latitude pine forest growing on sandy soil. *Agric. For. Meteorol.* **111**, 157–170 (2002).
75. J. Kurbatova, C. Li, A. Varlagin, X. Xiao, N. Vygodskaya, Modeling carbon dynamics in two adjacent spruce forests with different soil conditions in Russia. *Biogeosciences* **5**, 969–980 (2008).
76. J. Sagerfors, A. Lindroth, A. Grelle, L. Klemedtsson, P. Weslien, M. Nilsson, Annual CO_2 exchange between a nutrient-poor, minerotrophic, boreal mire and the atmosphere. *J. Geophys. Res. Biogeosci.* **113**, (2008).
77. C. Yi, D. Ricciuto, R. Li, J. Wolbeck, X. Xu, M. Nilsson, L. Aires, J. D. Albertson, C. Ammann, M. A. Arain, A. C. de Araujo, M. Aubinet, M. Aurela, Z. Barcza, A. Barr, P. Berbigier, J. Beringer, C. Bernhofer, A. T. Black, P. V. Bolstad, F. C. Bosveld, M. S. J. Broadmeadow, N. Buchmann, S. P. Burns, P. Cellier, J. Chen, J. Chen, P. Ciais, R. Clement, B. D. Cook, P. S. Curtis, D. B. Dail, E. Dellwik, N. Delpierre, A. R. Desai, S. Dore, D. Dragoni, B. G. Drake, E. Dufrêne, A. Dunn, J. Elbers, W. Eugster, M. Falk, C. Feigenwinter, L. B. Flanagan, T. Foken, J. Frank, J. Fuhrer, D. Gianelle, A. Goldstein, M. Goulden, A. Granier, T. Grünwald, L. Gu, H. Guo, A. Hammerle, S. Han, N. P. Hanan, L. Haszpra, B. Heinesch, C. Helfter, D. Hendriks, L. B. Hutley, A. Ibrom, C. Jacobs, T. Johansson, M. Jongen, G. Katul, G. Kiely, K. Klumpp, A. Knohl, T. Kolb, W. L. Kutsch, P. Lafleur, T. Laurila, R. Leuning, A. Lindroth, H. Liu, B. Loubet, G. Manca, M. Marek, H. A. Margolis, T. A. Martin, W. J. Massman, R. Matamala, G. Matteucci, H. McCaughey, L. Merbold, T. Meyers, M. Migliavacca, F. Miglietta, L. Misson, M. Mölder, J. Moncrieff, R. K. Monson, L. Montagnani, M. Montes-Helu, E. Moors, C. Moureaux, M. M. Mukelabai, J. W. Munger, M. Myklebust, Z. Nagy, A. Noormets, W. Oechel, R. Oren, S. G. Pallardy, U. Kyaw Tha Paw, J. S. Pereira, K. Pilegaard, K. Pintér, C. Pio, G. Pita, T. L. Powell, S. Rambal, J. T. Randerson, C. von Randow, C. Rebmann, J. Rinne, F. Rossi, N. Roulet, R. J. Ryel, J. Sagerfors, N. Saigusa, M. J. Sanz, G.-S. Mugnozza, H. P. Schmid, G. Seufert, M. Siqueira, J.-F. Soussana, G. Starr, M. A. Sutton, J. Tenhunen, Z. Tuba, J.-P. Tuovinen, R. Valentini, C. S. Vogel, J. Wang, S. Wang, W. Wang, L. R. Welp, X. Wen, S. Wharton, M. Wilkinson, C. A. Williams, G. Wohlfahrt, S. Yamamoto, G. Yu, R. Zampedri, B. Zhao, X. Zhao, Climate control of terrestrial carbon exchange across biomes and continents. *Environ. Res. Lett.* **5**, 034007 (2010).
78. S. Urbanski, C. Barford, S. Wofsy, C. Kucharik, E. Pyle, J. Budney, K. McKain, D. Fitzjarrald, M. Czikowsky, J. W. Munger, Factors controlling CO_2 exchange on timescales from hourly to decadal at Harvard Forest. *J. Geophys. Res. Biogeosci.* **112**, G02020 (2007).
79. M. L. Fischer, D. P. Billesbach, J. A. Berry, W. J. Riley, M. S. Torn, Spatiotemporal variations in growing season exchanges of CO_2, H_2O, and sensible heat in agricultural fields of the Southern Great Plains. *Earth Interact.* **11**, 1–21 (2007).
80. J. P. Jenkins, A. D. Richardson, B. H. Braswell, S. V. Ollinger, D. Y. Hollinger, M.-L. Smith, Refining light-use efficiency calculations for a deciduous forest canopy using simultaneous tower-based carbon flux and radiometric measurements. *Agric. For. Meteorol.* **143**, 64–79 (2007).
81. M. Migliavacca, M. Reichstein, A. D. Richardson, R. Colombo, M. A. Sutton, G. Lasslop, E. Tomelleri, G. Wohlfahrt, N. Carvalhais, A. Cescatti, M. D. Mahecha, L. Montagnani, D. Papale, S. Zaehle, A. Arain, A. Arneth, T. A. Black, A. Carrara, S. Dore, D. Gianelle, C. Helfter, D. Hollinger, W. L. Kutsch, P. M. Lafleur, Y. Nouvellon, C. Rebmann, H. R. Da Rocha, M. Rodeghiero, O. Roupsard, M.-T. Sebastià, G. Seufert, J.-F. Soussana, M. K. Van Der Molen, Semiempirical modeling of abiotic and biotic factors controlling ecosystem respiration across eddy covariance sites. *Glob. Chang. Biol.* **17**, 390–409 (2011).
82. D. E. Pataki, R. Oren, Species differences in stomatal control of water loss at the canopy scale in a mature bottomland deciduous forest. *Adv. Water Resour.* **26**, 1267–1278 (2003).
83. S. Dore, T. E. Kolb, M. Montes-Helu, B. W. Sullivan, W. D. Winslow, S. C. Hart, J. P. Kaye, G. W. Koch, B. A. Hungate, Long-term impact of a stand-replacing fire on ecosystem CO_2 exchange of a ponderosa pine forest. *Glob. Chang. Biol.* **14**, 1801–1820 (2008).
84. D. Y. Hollinger, J. Aber, B. Dail, E. A. Davidson, S. M. Goltz, H. Hughes, M. Y. Leclerc, J. T. Lee, A. D. Richardson, C. Rodrigues, N. A. Scott, D. Achuatavarier, J. Walsh, Spatial and temporal variability in forest-atmosphere CO_2 exchange. *Glob. Chang. Biol.* **10**, 1689–1706 (2004).
85. R. Oren, C.-I. Hsieh, P. Stoy, J. Albertson, H. R. Mccarthy, P. Harrell, G. G. Katul, Estimating the uncertainty in annual net ecosystem carbon exchange: Spatial variation in turbulent fluxes and sampling errors in eddy-covariance measurements. *Glob. Chang. Biol.* **12**, 883–896 (2006).
86. J.-H. Li, W. A. Dugas, G. J. Hymus, D. P. Johnson, C. R. Hinkle, B. G. Drake, B. A. Hungate, Direct and indirect effects of elevated CO_2 on transpiration from *Quercus myrtifolia* in a scrub-oak ecosystem. *Glob. Chang. Biol.* **9**, 96–105 (2003).
87. H. P. Schmid, C. S. B. Grimmond, F. Cropley, B. Offerle, H.-B. Su, Measurements of CO_2 and energy fluxes over a mixed hardwood forest in the mid-western United States. *Agric. For. Meteorol.* **103**, 357–374 (2000).

88. Y. Gu, K. N. Liou, Y. Xue, C. R. Mechoso, W. Li, Y. Luo, Climatic effects of different aerosol types in China simulated by the UCLA general circulation model. *J. Geophys. Res. Atmos.* **111**, D15201 (2006).
89. M. Reichstein, E. Falge, D. Baldocchi, D. Papale, M. Aubinet, P. Berbigier, C. Bernhofer, N. Buchmann, T. Gilmanov, A. Granier, T. Grünwald, K. Havránková, H. Ilvesniemi, D. Janous, A. Knohl, T. Laurila, A. Lohila, D. Loustau, G. Matteucci, T. Meyers, F. Miglietta, J.-M. Ourcival, J. Pumpanen, S. Rambal, E. Rotenberg, M. Sanz, J. Tenhunen, G. Seufert, F. Vaccari, T. Vesala, D. Yakir, R. Valentini, On the separation of net ecosystem exchange into assimilation and ecosystem respiration: Review and improved algorithm. *Glob. Chang. Biol.* **11**, 1424–1439 (2005).
90. R. K. Monson, A. A. Turnipseed, J. P. Sparks, P. C. Harley, L. E. Scott-Denton, K. Sparks, T. E. Huxman, Carbon sequestration in a high-elevation, subalpine forest. *Glob. Chang. Biol.* **8**, 459–478 (2002).
91. J. L. Deforest, A. Noormets, S. G. Mc Nulty, G. Sun, G. Tenney, J. Chen, Phenophases alter the soil respiration–temperature relationship in an oak-dominated forest. *Int. J. Biometeorol.* **51**, 135–144 (2006).
92. K. J. Davis, P. S. Bakwin, C. Yi, B. W. Berger, C. Zhao, R. M. Teclaw, J. G. Isebrands, The annual cycles of CO_2 and H_2O exchange over a northern mixed forest as observed from a very tall tower. *Glob. Chang. Biol.* **9**, 1278–1293 (2003).
93. R. L. Scott, G. D. Jenerette, D. L. Potts, T. E. Huxman, Effects of seasonal drought on net carbon dioxide exchange from a woody-plant-encroached semiarid grassland. *J. Geophys. Res. Biogeosci.* **114**, G04004 (2009).
94. A. R. Desai, P. V. Bolstad, B. D. Cook, K. J. Davis, E. V. Carey, Comparing net ecosystem exchange of carbon dioxide between an old-growth and mature forest in the upper Midwest, USA. *Agric. For. Meteorol.* **128**, 33–55 (2005).
95. C. M. Gough, C. S. Vogel, H. P. Schmid, H.-B. Su, P. S. Curtis, Multi-year convergence of biometric and meteorological estimates of forest carbon storage. *Agric. For. Meteorol.* **148**, 158–170 (2008).
96. B. D. Cook, K. J. Davis, W. Wang, A. Desai, B. W. Berger, R. M. Teclaw, J. G. Martin, P. V. Bolstad, P. S. Bakwin, C. Yi, W. Heilman, Carbon exchange and venting anomalies in an upland deciduous forest in northern Wisconsin, USA. *Agric. For. Meteorol.* **126**, 271–295 (2004).
97. R. L. Scott, E. P. Hamerlynck, G. D. Jenerette, M. S. Moran, G. A. Barron-Gafford, Carbon dioxide exchange in a semidesert grassland through drought-induced vegetation change. *J. Geophys. Res. Biogeosci.* **115**, G03026 (2010).
98. M. Falk, S. Wharton, M. Schroeder, S. Ustin, U. K. Paw, Flux partitioning in an old-growth forest: Seasonal and interannual dynamics. *Tree Physiol.* **28**, 509–520 (2008).
99. P. L. Shi, X. Sun, L. Xu, X. Zhang, Y. He, D. Zhang, G. Yu, Net ecosystem CO_2 exchange and controlling factors in a steppe––*Kobresia* meadow on the Tibetan Plateau. *Sci. China Ser. D* **49**, 207–218 (2006).
100. G. R. Yu, L.-M. Zhang, X.-M. Sun, Y.-L. Fu, X.-F. Wen, Q.-F. Wang, S.-G. Li, C.-Y. Ren, X. Song, Y.-F. Liu, S.-J. Han, J.-H. Yan, Environmental controls over carbon exchange of three forest ecosystems in eastern China. *Glob. Chang. Biol.* **14**, 2555–2571 (2008).
101. T. Kato, Y. Tang, S. Gu, X. Cui, M. Hirota, M. du, Y. Li, X. Zhao, T. Oikawa, Carbon dioxide exchange between the atmosphere and an alpine meadow ecosystem on the Qinghai–Tibetan Plateau, China. *Agric. For. Meteorol.* **124**, 121–134 (2004).
102. Y.-L. Fu, G.-R. Yu, X.-M. Sun, Y.-N. Li, X.-F. Wen, L.-M. Zhang, Z.-Q. Li, L. Zhao, Y.-B. Hao, Depression of net ecosystem CO_2 exchange in semi-arid *Leymus chinensis* steppe and alpine shrub. *Agric. For. Meteorol.* **137**, 234–244 (2006).
103. N. Saigusa, S. Yamamoto, S. Murayama, H. Kondo, Inter-annual variability of carbon budget components in an AsiaFlux forest site estimated by long-term flux measurements. *Agric. For. Meteorol.* **134**, 4–16 (2005).
104. F. Rubel, M. Kottek, Observed and projected climate shifts 1901-2100 depicted by world maps of the Köppen-Geiger climate classification. *Meteorol. Z.* **19**, 135–141 (2010).
105. M. C. Hansen, R. S. Defries, J. R. G. Townshend, R. Sohlberg, Global land cover classification at 1 km spatial resolution using a classification tree approach. *Int. J. Remote Sens.* **21**, 1331–1364 (2010).
106. C. Beier, B. A. Emmett, J. Peñuelas, I. K. Schmidt, A. Tietema, M. Estiarte, P. Gundersen, L. Llorens, T. Riis-Nielsen, A. Sowerby, A. Gorissen, Carbon and nitrogen cycles in European ecosystems respond differently to global warming. *Sci. Total Environ.* **407**, 692–697 (2008).
107. D. R. Bronson, S. T. Gower, M. Tanner, S. Linder, I. Van Herk, Response of soil surface CO_2 flux in a boreal forest to ecosystem warming. *Glob. Chang. Biol.* **14**, 856–867 (2008).
108. F. Hagedorn, M. Martin, C. Rixen, S. Rusch, P. Bebi, A. Zürcher, R. T. W. Siegwolf, S. Wipf, C. Escape, J. Roy, S. Hättenschwiler, Short-term responses of ecosystem carbon fluxes to experimental soil warming at the Swiss alpine treeline. *Biogeochemistry* **97**, 7–19 (2010).
109. X. Lu, J. Fan, Y. Yan, X. Wang, Responses of soil CO_2 fluxes to short-term experimental warming in alpine steppe ecosystem, northern tibet. *PLOS ONE* **8**, e59054 (2013).
110. F. L. Marchand, I. Nijs, H. J. de Boeck, F. Kockelbergh, S. Mertens, L. Beyens, Increased turnover but little change in the carbon balance of high-arctic tundra exposed to whole growing season warming. *Arct. Antarct. Alp. Res.* **36**, 298–307 (2004).
111. P. J. McHale, M. J. Mitchell, F. P. Bowles, Soil warming in a northern hardwood forest: Trace gas fluxes and leaf litter decomposition. *Can. J. For. Res.* **28**, 1365–1372 (1998).
112. W. T. Peterjohn, J. M. Melillo, P. A. Steudler, K. M. Newkirk, F. P. Bowles, J. D. Aber, Responses of trace gas fluxes and N availability to experimentally elevated soil temperatures. *Ecol. Appl.* **4**, 617–625 (1994).
113. C. Poll, S. Marhan, F. Back, P. A. Niklaus, E. Kandeler, Field-scale manipulation of soil temperature and precipitation change soil CO2 flux in a temperate agricultural ecosystem. *Agric. Ecosyst. Environ.* **165**, 88–97 (2013).
114. A. Schindlbacher, S. Zechmeister-Boltenstern, R. Jandl, Carbon losses due to soil warming: Do autotrophic and heterotrophic soil respiration respond equally? *Glob. Chang. Biol.* **15**, 901–913 (2009).
115. V. Suseela, J. S. Dukes, The responses of soil and rhizosphere respiration to simulated climatic changes vary by season. *Ecology* **94**, 403–413 (2013).
116. Z. Xu, C. Wan, P. Xiong, Z. Tang, R. Hu, G. Cao, Q. Liu, Initial responses of soil CO2 efflux and C, N pools to experimental warming in two contrasting forest ecosystems, Eastern Tibetan Plateau, China. *Plant Soil* **336**, 183–195 (2010).
117. X. Zhou, R. A. Sherry, Y. An, L. L. Wallace, Y. Luo, Main and interactive effects of warming, clipping, and doubled precipitation on soil CO2 efflux in a grassland ecosystem. *Glob. Biogeochem. Cycles* **20**, GB1003 (2006).
118. X. Zhou, S. Wan, Y. Luo, Source components and interannual variability of soil CO2 efflux under experimental warming and clipping in a grassland ecosystem. *Glob. Chang. Biol.* **13**, 761–775 (2007).
119. S. Wan, R. J. Norby, J. Ledford, J. F. Weltzin, Responses of soil respiration to elevated CO2, air warming, and changing soil water availability in a model old-field grassland. *Glob. Chang. Biol.* **13**, 2411–2424 (2007).
120. M. Aguilos, K. Takagi, N. Liang, Y. Watanabe, M. Teramoto, S. Goto, Y. Takahashi, H. Mukai, K. Sasa, Sustained large stimulation of soil heterotrophic respiration rate and its temperature sensitivity by soil warming in a cool-temperate forested peatland. *Tellus Ser. B Chem. Phys. Meteorol.* **65**, 20792 (2013).
121. G. Fu, Z. X. Shen, X. Z. Zhang, C. Q. Yu, Y. T. Zhou, Y. L. Li, P. W. Yang, Response of ecosystem respiration to experimental warming and clipping at daily time scale in an alpine meadow of Tibet. *J. Mt. Sci.* **10**, 455–463 (2013).
122. Z.-M. Zhong, Z.-X. Shen, G. Fu, Response of soil respiration to experimental warming in a highland barley of the Tibet. *Springerplus* **5**, 137 (2016).
123. J. Chen, X. Zhou, T. Hruska, J. Cao, B. Zhang, C. Liu, M. Liu, S. Shelton, L. Guo, Y. Wei, J. Wang, S. Xiao, P. Wang, Asymmetric diurnal and monthly responses of ecosystem carbon fluxes to experimental warming. *Clean* **45**, 1600557 (2017).
124. P. E. Eliasson, R. E. McMurtrie, D. A. Pepper, M. Stromgren, S. Linder, G. I. Agren, The response of heterotrophic CO2 flux to soil warming. *Glob. Chang. Biol.* **11**, 167–181 (2005).
125. M. StrÖMgren, S. Linder, Effects of nutrition and soil warming on stemwood production in a boreal Norway spruce stand. *Glob. Chang. Biol.* **8**, 1194–1204 (2002).
126. C. Fang, J.-S. Ye, Y. Gong, J. Pei, Z. Yuan, C. Xie, Y. Zhu, Y. Yu, Seasonal responses of soil respiration to warming and nitrogen addition in a semi-arid alfalfa-pasture of the Loess Plateau, China. *Sci. Total Environ.* **590–591**, 729–738 (2017).
127. A. B. Jansen-Willems, G. J. Lanigan, L. Grünhage, C. Müller, Carbon cycling in temperate grassland under elevated temperature. *Ecol. Evol.* **6**, 7856–7868 (2016).
128. X. Lin, Z. Zhang, S. Wang, Y. Hu, G. Xu, C. Luo, X. Chang, J. Duan, Q. Lin, B. Xu, Y. Wang, X. Zhao, Z. Xie, Response of ecosystem respiration to warming and grazing during the growing seasons in the alpine meadow on the Tibetan plateau. *Agric. For. Meteorol.* **151**, 792–802 (2011).
129. C. Luo, G. Xu, Z. Chao, S. Wang, X. Lin, Y. Hu, Z. Zhang, J. Duan, X. Chang, A. Su, Y. Li, X. Zhao, M. Du, Y. Tang, B. Kimball, Effect of warming and grazing on litter mass loss and temperature sensitivity of litter and dung mass loss on the Tibetan plateau. *Glob. Chang. Biol.* **16**, 1606–1617 (2010).
130. W. Liu, Z. H. E. Zhang, S. Wan, Predominant role of water in regulating soil and microbial respiration and their responses to climate change in a semiarid grassland. *Glob. Chang. Biol.* **15**, 184–195 (2009).
131. T. Liu, S. Liu, S. Wang, J. Luan, H. Wang, Differential responses of soil respiration to soil warming and experimental throughfall reduction in a transitional oak forest in central China. *Agric. For. Meteorol.* **226–227**, 186–198 (2016).
132. N. J. Noh, S. J. Lee, W. Jo, S. Han, T. K. Yoon, H. Chung, H. Muraoka, Y. Son, Effects of experimental warming on soil respiration and biomass in Quercus variabilis Blume and Pinus densiflora Sieb. et Zucc. seedlings. *Ann. For. Sci.* **73**, 533–545 (2016).
133. N.-J. Noh, M. Kuribayashi, T. M. Saitoh, T. Nakaji, M. Nakamura, T. Hiura, H. Muraoka, Responses of soil, heterotrophic, and autotrophic respiration to experimental open-field soil warming in a cool-temperate deciduous forest. *Ecosystems* **19**, 504–520 (2016).
134. B. Pajari, *Nutrient Uptake and Cycling in Forest Ecosystems: Proceedings of the CEC/IUFRO Symposium Nutrient Uptake and Cycling in Forest Ecosystems Halmstad, Sweden, June, 7–10, 1993*, L. O. Nilsson, R. F. Hüttl, U. T. Johansson, Eds. (Springer Netherlands, Dordrecht, 1995), pp. 563–570.

135. J. G. Vogel, D. Bronson, S. T. Gower, E. A. G. Schuur, The response of root and microbial respiration to the experimental warming of a boreal black spruce forest. *Can. J. For. Res.* **44**, 986–993 (2014).
136. G. Xu, H. Jiang, Y. Zhang, H. Korpelainen, C. Li, Effect of warming on extracted soil carbon pools of Abies faxoniana forest at two elevations. *For. Ecol. Manag.* **310**, 357–365 (2013).
137. Q. Zhong, Q. Du, J. Gong, C. Zhang, K. Wang, Effects of in situ experimental air warming on the soil respiration in a coastal salt marsh reclaimed for agriculture. *Plant Soil* **371**, 487–502 (2013).

Acknowledgments: We thank the FLUXNET dataset, the ESGF Search Portal, and the KNMI Climate Explorer for providing model outputs of warming scenarios. **Funding**: This work was financially supported by the Second Tibetan Plateau Scientific Expedition and Research Program (STEP) (no. 2019QZKK1002); the Strategic Priority Research Program of the Chinese Academy of Sciences (nos. XDA20050102 and XDA19070303), the National Natural Science Foundation of China (no. 41807331), and the National Key Research and Development Program (nos. 2016YFC0502001 and 2017YFA0604801). I.A.J. is supported by the European Research Council Synergy (no. ERC-2013-SyG-610028 IMBALANCE-P). A.R.D. acknowledges support from the U.S. Department of Energy Ameriflux Network Management Project. I.M. acknowledges funding from the Academy of Finland Flagship (grant no. 337549) and ICOS-Finland by the University of Helsinki. **Author contributions:** X. Zhang, B.N., I.A.J., and S.P. conceived the method. B.N. and X. Zhang. synthesized data, performed the analysis, and prepared figures. B.N., X. Zhang, S.P., and I.A.J. drafted the manuscript. All authors provided data for the analysis, discussed the results and implications, and commented on the manuscript at all stages. **Competing interests:** The authors declare that they have no competing interests. **Data and materials availability:** All data needed to evaluate the conclusions in the paper are present in the paper and/or the Supplementary Materials. Specifically, the EC-based measurements that support the findings of this study are available from the FLUXNET dataset (https://fluxnet.org/). The site-specific warming scenarios that support the findings of this study are also publicly available at the KNMI Climate Explorer (https://climexp.knmi.nl). The CMIP5 model outputs are available at the CEDA ESGF Search Portal (https://esgf-node.llnl.gov/search/cmip5/). Additional data related to this paper may be requested from the authors (niub@igsnrr.ac.cn and zhangxz@igsnrr.ac.cn).

Submitted 11 May 2020
Accepted 24 February 2021
Published 9 April 2021
10.1126/sciadv.abc7358

Citation: B. Niu, X. Zhang, S. Piao, I. A. Janssens, G. Fu, Y. He, Y. Zhang, P. Shi, E. Dai, C. Yu, J. Zhang, G. Yu, M. Xu, J. Wu, L. Zhu, A. R. Desai, J. Chen, G. Bohrer, C. M. Gough, I. Mammarella, A. Varlagin, S. Fares, X. Zhao, Y. Li, H. Wang, Z. Ouyang, Warming homogenizes apparent temperature sensitivity of ecosystem respiration. *Sci. Adv.* **7**, eabc7358 (2021).

Warming homogenizes apparent temperature sensitivity of ecosystem respiration

Ben Niu, Xianzhou Zhang, Shilong Piao, Ivan A. Janssens, Gang Fu, Yongtao He, Yangjian Zhang, Peili Shi, Erfu Dai, Chengqun Yu, Jing Zhang, Guirui Yu, Ming Xu, Jianshuang Wu, Liping Zhu, Ankur R. Desai, Jiquan Chen, Gil Bohrer, Christopher M. Gough, Ivan Mammarella, Andrej Varlagin, Silvano Fares, Xinquan Zhao, Yingnian Li, Huiming Wang and Zhu Ouyang

Sci Adv **7** (15), eabc7358.
DOI: 10.1126/sciadv.abc7358